Hybrid Multimodal Deformable Registration with a Data-Driven Deformation Prior

Yongning Lu[1,2], Ying Sun[2], Rui Liao[4], and Sim Heng Ong[1,2,3]

[1] NUS Graduate School for Integrative Sciences and Engineering, NUS, Singapore
[2] Department of Electrical and Computer Engineering, NUS, Singapore
[3] Department of Bioengineering, NUS, Singapore
[4] Siemens Corporation, Corporate Research and Technology

Abstract. Deformable registration for images with different contrast-enhancement and hence different structure appearance is extremely challenging due to the ill-posed nature of the problem. Utilizing prior anatomical knowledge is thus necessary to eliminate implausible deformations. Landmark constraints and statistically constrained models have shown encouraging results. However, these methods do not utilize the segmentation information that may be readily available. In this paper, we explore the possibility of utilizing such information. We propose to generate an anatomical correlation-regularized deformation field prior by registration of point sets using mixture of Gaussians based on a thin-plate spline parametric model. The point sets are extracted from the segmented object surface and no explicit landmark matching is required. The prior is then incorporated with an intensity-based similarity measure in the deformable registration process using the variational framework. The proposed prior does not require any training data set thus excluding any inter-subject variations compared to learning-based methods. In the experiments, we show that our method increases the registration robustness and accuracy on 12 sets of TAVI patient data, 8 myocardial perfusion MRI sequences, and one simulated pre- and post- tumor resection MRI.

1 Introduction

Image registration helps the clinicians to combine the image information acquired from different modalities, different time points, or pre- and post- contrast-enhancement for better evaluation. Many of the medical applications rely on the technique of image registration, ranging from examination of disease progression, to the usage of augmented reality in the minimal-invasive interventions. For some cases, rigid/affine registration may be sufficient; however, in many cases, deformable registration is needed to compensate for local movements.

Deformable registration is inherently ill-posed and under-constrained from the mathematical point of view. It becomes more challenging when dealing with different structure appearances due to different levels of contrast-enhancement between two images. This problem widely exists in the field of medical image registration, e.g., registration of the perfusion cardiac image in the wash

C.A. Linte et al. (Eds.): MIAR/AE-CAI 2013, LNCS 8090, pp. 45–54, 2013.

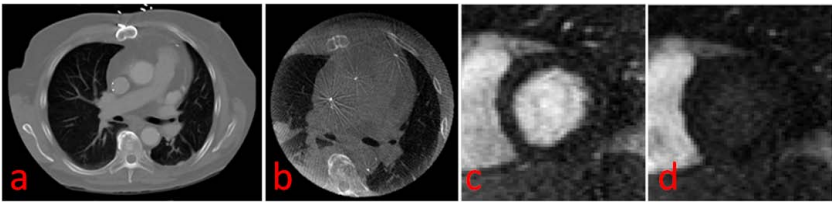

Fig. 1. Structure appearance may be largely different due to different levels of contrast-enhancement. (a) and (b) is a pair of images from pre-operative contrast-enhanced CT and intra-operative non-contrast-enhanced C-arm CT for TAVI procedure. (c) and (d) is a pair of images from a perfusion cardiac sequence at different phases.

in/out phases, and 3D/3D registration of pre-operative contrast-enhanced CT and intra-operative non-contrast-enhanced C-arm CT images. In these cases, purely relying on the intensity information produces anatomically implausible deformation. To facilitate the deformable registration process, landmark constraints were proposed to increase the registration accuracy and robustness [1,2,3]. These methods added a penalty term to penalize the correspondence pairs from moving too far apart, therefore, accurate correspondence matching is crucial. Incorporating the knowledge of statistical analysis on shape and displacement field variability to the image registration process is another popular approach [4,5]. Xue et al. [6] tackled the problem of high dimensional statistical deformation models (SDMs) using wavelet based decompositions. Despite the promising results, training the SDMs suffers from the curse of dimensionality, and how to select the training data to represent the population remains unclear. Recently, Lu et al. proposed the structural-encoded mutual information (SMI) [7] which emphasizes the structures that commonly exist in both images. And they further incorporated the rigid spine motion into their proposed application. Incorporating the rigid motion of spine movement is clearly adhoc: it cannot be applied to images which do not contain spine and/or have deformable motion. Among the aforementioned methods, one important and potentially readily available information is missing and may be utilized — the segmentation of some dominant and common objects in the images. The motion of these segmented objects could be modeled and may greatly improve the registration accuracy. In addition, from the clinical workflow perspective, this segmentation may be needed for diagnosis and guidance purpose alone, and as a result, utilization of the available segmentation results does not impose additional requirement for the purpose of image registration.

In this paper, we propose a novel hybrid deformable registration framework for multimodal image registration. The proposed method targets at image pairs that have different structure appearance. Theoretically it is a generalization of the method in [7] to deal with general structures containing deformable motion by utilizing available segmentations. A data-driven anatomical correlation-regularized deformation field prior is generated by registration of the point sets from the segmented objects using mixture of Gaussians based on a TPS model. The proposed cost function combines the high-level knowledge from the anatomical

correlation-regularized deformation field and low-level intensity statistical information. Therefore, the segmentation does not need to be complete, and may focus only on the dominant structures to provide regularization on the deformation field. The fine-level registration is largely driven by the image intensity, which leads to a much more accurate registration compared to simple warping using the segmentation results alone.

2 Method

2.1 Anatomical Correlation-Regularized Deformation Field Prior

Despite the popularity of landmark-based image registration techniques, for many applications, it is very difficult to find exact/accurate landmark correspondences from the images automatically due to the poor image quality. However, relatively good segmentation of some dominant objects in these image is still possible. In our work, we assume that the segmentation of some dominant objects is given *a priori*, and the point sets are extracted from the object surfaces. The distribution of the points were modeled using mixture of Gaussians. Then we use the method in [8] to register the sampled point sets efficiently without establishing explicit point correspondences. We generate an anatomical correlation-regularized deformation field prior $\boldsymbol{v}$ using TPS model by optimizing:

$$E_{TPS}(\boldsymbol{v}) = \int (f_{\boldsymbol{v}} - g)^2 d\boldsymbol{x} + \lambda E_{bend}(\boldsymbol{v}), \tag{1}$$

where $f_{\boldsymbol{v}}$ is the distribution representing the transformed point set warped by $\boldsymbol{v}$, and g is the distribution of the reference point set. A small λ ensures that the TPS approximate local deformations well [9]. In our work, we choose λ to be 0.001. $E_{bend}(\boldsymbol{v})$ is the bending energy of the TPS. We refer the readers to [10] for more details of the TPS warping.

TPS is chosen to represent the underlying transformation model due to its nice properties, including its smoothness, no free parameters to tune manually, closed-form solutions for both warping and parameter estimation, and physical explanation for its energy function [3,11]. Moreover, the point sets are modeled using mixture of Gaussians for the purpose of efficient and robust registration [8]. Registration of models of mixtures of Gaussians may not be highly accurate at the edges, compared to other computationally-expensive landmark-based registration methods that focus on point-to-point matching. However, the deformation prior generated from the point sets registration results is sufficient to provide a high-level knowledge of the plausible deformation field. Note that, different from spline-based optimization schemes in other hybrid methods, we only used TPS to approximate the segmentation-based registration results. Furthermore, the distribution of the point sets obtained from segmentation are modeled as mixture of Gaussians, thus no iterative volume intensity interpolation is involved which leads to much higher computation efficiency. In our hybrid registration method, the registration will be largely driven by image intensity in regions where structural information is rich. In contrast, in regions where the

structures do not match (e.g. due to different levels of contrast enhancement), the registration will be mainly regularized by the generated prior deformation field.

2.2 Cost Function

The proposed cost function E combines a data term E_{s} and a penalty term E_{p}, and the weight α balances the influences of the two terms:

$$E(\boldsymbol{u}) = E_{\mathrm{s}}(\boldsymbol{u}) + \alpha E_{\mathrm{p}}(\boldsymbol{u}), \tag{2}$$

where $\boldsymbol{u}$ is the deformation field. The data term E_{s} aims to maximize the low-level intensity statistical dependency of the two images, whereas the penalty term E_{p} discourages certain implausible deformations deviated from the prior deformation field, and the weight term α is set to 0.1.

Data Term. Intensity-based similarity measures are widely reported. Popular similarity measures include mutual information, normalized mutual information, correlation ratio, and cross correlation etc. As the main focus of our paper is to introduce a prior deformation field into the deformable registration framework, we would not specify the intensity-based similarity measure. The readers are free to choose any of the intensity-based similarity measures which varies by different applications, and can then be combined with the proposed prior deformation field.

Penalty from Prior Deformation Field. Optimizing (1) provides a data-driven prior deformation field $\boldsymbol{v}$, and we want the prior deformation field $\boldsymbol{v}$ to guide the deformable registration process. The penalty term is defined as:

$$E_{\mathrm{p}}(\boldsymbol{u}) = -\int_{\Omega} w(\boldsymbol{x})||\boldsymbol{u}(\boldsymbol{x}) - \boldsymbol{v}(\boldsymbol{x})||^2 d\boldsymbol{x}. \tag{3}$$

$\boldsymbol{x}$ is the location of the pixel/voxel. A local weight term $w(\boldsymbol{x})$ is included in the penalty term. $w(\boldsymbol{x})$ is assigned to be large at the structure mismatching area, and small at the area where structure information is rich and corresponds well in the two images.

2.3 Optimization

To optimize the cost function, we follow the variational framework proposed by Hermosillo et al. [12], which exhibits nice properties in terms of accuracy, capture range, and computational efficiency compared to the parametric deformable models. In particular, following the notation in [12], the gradient for variational minimization of the cost function is derived as:

$$\frac{\partial \boldsymbol{u}}{\partial t} = -\frac{\partial E(\boldsymbol{u})}{\partial \boldsymbol{u}} = -\frac{\partial E_{\mathrm{s}}(\boldsymbol{u})}{\partial \boldsymbol{u}} - \alpha \frac{\partial E_{\mathrm{p}}(\boldsymbol{u})}{\partial \boldsymbol{u}}. \tag{4}$$

As $\frac{\partial E_{\mathrm{s}}}{\partial \boldsymbol{u}}$ varies according to the choice of the data term, in this section, we only provide the derivation of $\frac{\partial E_{\mathrm{p}}(\boldsymbol{u})}{\partial \boldsymbol{u}(\boldsymbol{x})}$.

$$\frac{\partial E_{\mathrm{p}}(\boldsymbol{u})}{\partial \boldsymbol{u}(\boldsymbol{x})} = 2w(\boldsymbol{x})(\boldsymbol{u}(\boldsymbol{x}) - \boldsymbol{v}(\boldsymbol{x})), \tag{5}$$

The use of the weight term $w(\boldsymbol{x})$ leads to desirable properties while updating the deformation field at each iteration. Specifically, at the locations with mismatching structures, $w(\boldsymbol{x})$ is large. These areas usually produce large registration error when solely relying on the data term, so we highly rely on the penalty term (i.e. the deformation prior) to guide the registration process in these areas. On the other hand, at the locations where the structures appear in both images, $w(\boldsymbol{x})$ is small, therefore, the registration process relies more on the data term. Fast Gaussian filtering [13] is applied at each iteration to regularize the registration process.

2.4 Implementation

Our implementation is advanced with efficient filtering and fully parallelized. A multi-resolution scheme is deployed to speed up the registration process and reduce the chance of the optimization being trapped in the local minimum during the energy minimization process. For a typical 3D volume of 512×512×100, the entire registration process takes around 4 minutes for a dual core CPU, compared to 105 minutes for a B-spline based implementation reported in EMPIRE10 Challenge [14].

3 Experiments

3.1 Pre-operative CT and Non-contrast-enhanced C-arm CT

Registration of pre-operative contrast-enhanced CT and non-contrast-enhanced C-arm CT eliminates the need for acquiring contrast-enhanced C-arm CT, which is harmful to trans-catheter aortic valve implantation (TAVI) patients with kidney impairments. Our first experiment is performed on 12 TAVI patients who had undergone both CT and contrast-enhanced C-arm CT scans.

Experimental Setup. Following the same procedure in [7], we create non-contrast-enhanced C-arm CT volumes from the contrast-enhanced C-arm CT. The contrasted aortic area in the C-arm CT is replaced by intensities generated from a Gaussian distribution with mean equal to the heart area. The generated volume is visually indifferent from real non-contrast-enhanced C-arm CT volume acquired clinically. Thus we are essentially matching the CT with the non-contrast-enhanced C-arm CT with known ground truth. In this experiment, lung segmentation and rough spine segmentation can be obtained using the

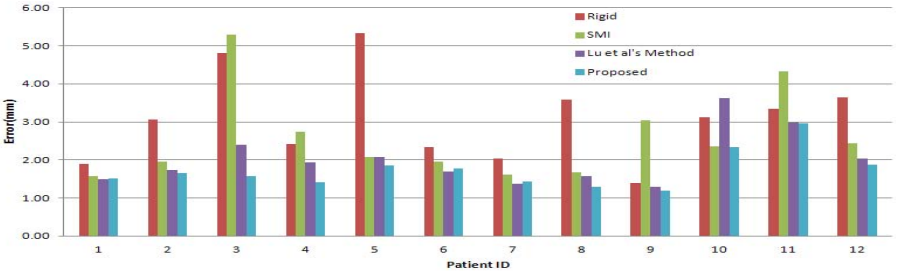

Fig. 2. Mesh-to-mesh error for 12 patients, using different registration methods

Fig. 3. Registration results, (a) Rigid (b) Deformable using SMI (c) Lu et al.'s method (d) The proposed method

methods from [15] and [16]. The point sets are sampled from the lung surface and the spine area with equal spacing. $w(\boldsymbol{x})$ is defined as:

$$w(\boldsymbol{x}) = \exp(-(\frac{d_{\text{spine}}(\boldsymbol{x})}{W})) + (1 - \exp(-(\frac{d_{\text{lung}}(\boldsymbol{x})}{W}))), \tag{6}$$

where d_{lung} and d_{spine} are the distance maps to the surfaces of the lung and spine respectively. W is set to 2.25 cm to control the effective confidence region. $w(\boldsymbol{x})$ gives higher weight to the region away from the lung surface because in these textureless regions, the deformation prior is the main driving force. Similarly, in the spine region, the derived prior is more reliable and thus a higher weight is given. We use SMI as the data term as proposed in [7].

Results. We measure the mesh-to-mesh distance by calculating the distance between the points on surface mesh of the aortic root from CT to the closest point on the ground truth mesh from the C-arm CT (Fig. 2). We validate on the aortic root because it is the most important anatomical feature for guidance purpose during TAVI. The errors are 3.08 ± 1.17 mm, 2.59 ± 1.15 mm, 2.01 ± 0.69 mm and 1.74 ± 0.50 mm for rigid-body registration, deformable registration using SMI, Lu et al.'s method [7] and our proposed method, respectively. The results show that deformable registration is necessary to compensate for the residual motion after

rigid registration. Compared to the intensity-based SMI, our method and Lu et al.'s method show the importance of incorporating anatomical knowledge into the deformable registration framework. Clinically, a registration error below 2.5 mm is deemed acceptable. Compared to Lu et al.'s method, we improve the result for patient 3 from borderline acceptable to very accurate, and furthermore, the result for patient 10 is improved from clinically not acceptable to applicable. We further perform a paired t-test between these two methods, and the two-tailed P value equals to 0.0411, showing that the proposed method is statistically significantly better than Lu et al.'s method. This is largely attributed to the proposed deformation prior, which is able to model the deformable heart motion, instead of simple rigid-body motion in the spine area as proposed in [7]. One registration example is shown in Fig. 3. The proposed method produces the most accurate registration result at the targeted area – the aortic root (red contours). Furthermore, the anatomical structure at the heart area is nicely preserved, thanks to the incorporated deformation prior. We can see that intensity-based method fails badly because of the large area of mismatched structures. Although Lu et al.'s method performs well around the spine and heart surface (yellow contours), the registration result at the heart area is not clinically meaningful, e.g. the myocardium (green contours) is badly distorted.

3.2 Myocardial Perfusion MRI

We perform our second set of experiment on 8 myocardial perfusion MRI sequences. Due to the intensity change caused by the contrast enhancement, registration of myocardial perfusion MRI is considered as multimodal.

Experimental Setup. We select a floating frame which has the best contrast in the sequence, and the selected floating frame is registered to every frame of the sequence. In this experiment, we can obtain the epicardium segmentation

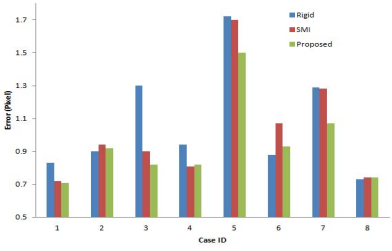

Fig. 4. Quantitative comparison of the registration errors (in *pixel*) obtained by rigid registration, SMI and the proposed method.

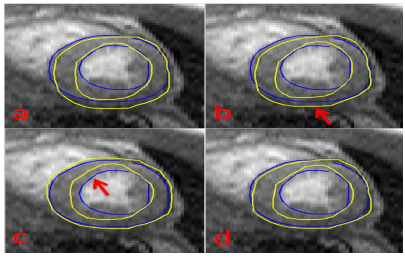

Fig. 5. Registration results (a) Rigid. (b) SMI. (c) Simple warping using the deformation prior. (d) Proposed method. Yellow and blue lines are the propogated and the ground truth contour.

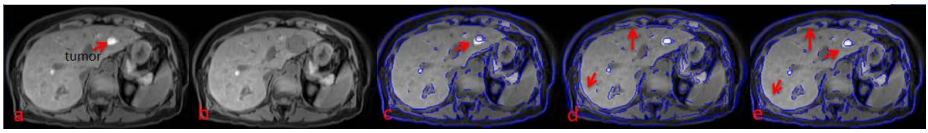

Fig. 6. (a) Pre-operative MRI. (b) Simulated post-operative MRI. (c), (d) and (e) are the registration results obtained by SMI, simple warping using the deformation prior, and the proposed method, respectively.

using [17]. The point sets are sampled from the epicardium outline with equal spacing. Similar to (6), $w(\boldsymbol{x})$ is a distance function to the segmented epicardium. The information of epicardium segmentation is thus implicitly embedded into the registration process. Again, SMI is used as the data term.

Results. For our data set, myocardial contours (epicardium and endocardium) of all the slices were drawn by a cardiologist. These contours serve as the ground truth. We calculated the root mean square distance from the ground truth to the propagated contours. The comprehensive comparison of each sequence can be found in Fig. 4. The paired t-test indicates that our hybrid method is statistically significantly better than the intensity-based method with P value equaling to 0.0263. We demonstrate the result using an example shown in Fig. 5, the main deficiency of the intensity-based and simple warping is emphasized using the red arrows. It is shown that intensity-based registration does not perform well in the homogeneous area because of the lack of structure information, while simple warping using the deformation prior results in noticeable registration errors at the structure-rich areas as the intensity information is ignored. In comparison, by combining the strength of both intensity-based and segmentation-based methods, our hybrid method produecs the best result. Note that Lu et al's method [7] is not applicable to this data due to the fact that there is no spine and the motion prior is non-rigid.

3.3 Simulated Pre- and Post- liver Tumor Resection MRI

The proposed hybrid method could be potentially applied to another category of registration problems with mismatching structures, i.e., registration between volumes of pre- and post- tumor resection. In this experiment, the registration is performed on pre-operative MRI and simulated post-operative MRI.

Experimental Setup. We simulated a post tumor resection image based on the pre-operative MRI. Then we artificially deform the pre-operative MRI, and registration is performed between the deformed pre-opeartive MRI and the simulated post-operative MRI. $w(\boldsymbol{x})$ is one at the resected area and zero otherwise. SMI is used as data term, where we do not count the statistics in the resected area. The deformation of the resected area solely relies on the regularization.

We assume the liver segmentation is available, and the point set is extracted from the liver surface.

Results. Here we get the qualitative preliminary results using one data set as shown in Fig. 6. Again, we use the arrows to emphasize the regions where intensity-based and simple warping using segmentation do perform well. Qualitatively, intensity-based registration does not perform well in the resected area, and simple warping using the liver segmentation does not preserve the detailed structures well. The proposed hybrid method guides the registration using the deformation prior at the resected area, while at the rest of the area, intensity-based method dominates. By combining the strength of both, the hybrid method achieves the best registration result as demonstrated in Fig. 6.

4 Discussion and Conclusion

In this paper, we present a hybrid multimodal deformable registration framework with a data-driven deformation prior. The proposed method addresses registration of images with different structure appearance due to different levels of contrast medium, and is validated on both TAVI and perfusion MR data. In addition, preliminary results show that the proposed method can also be applied to registration of pre- and post- tumor resection images. The experimental results demonstrate the superiority of the proposed method compared to intensity-based method and simple warping using segmentation. Furthermore, we derived the analytical solution for optimization under the variational framework which is computationally efficient. The main limitation of our method is the availability of the segmentation information. For our algorithm, we do not require very accurate segmentation result to generate the deformation prior to guide the registration process. Therefore, we can make use of the available segmentation algorithms to achieve the rough segmentation. Our algorithm is not applicable to images that no segmentation is available. In the future, we plan to apply the algorithm to more clinical data sets. We will also study how different segmentations will affect the registration results.

References

1. Sorzano, C.O., Thevenaz, P., Unser, M.: Elastic registration of biological images using vector-spline regularization. TBME 52, 652–663 (2005)
2. Papademetris, X., Jackowski, A., Schultz, R., Staib, L., Duncan, J.: Integrated intensity and point-feature nonrigid registration. In: Barillot, C., Haynor, D.R., Hellier, P. (eds.) MICCAI 2004. LNCS, vol. 3216, pp. 763–770. Springer, Heidelberg (2004)
3. Mitra, J., Kato, Z., Martí, R., Oliver, A., Lladó, X., Sidibé, D., Ghose, S., Vilanova, J., Comet, J., Meriaudeau, F.: A spline-based non-linear diffeomorphism for multimodal prostate registration. MIA (2012)
4. Wang, Y., Staib, L., et al.: Physical model-based non-rigid registration incorporating statistical shape information. MIA 4, 7–20 (2000)

5. Rueckert, D., Frangi, A., Schnabel, J.: Automatic construction of 3-D statistical deformation models of the brain using nonrigid registration. TMI 22, 1014–1025 (2003)
6. Xue, Z., Shen, D., Davatzikos, C., et al.: Statistical representation of high-dimensional deformation fields with application to statistically constrained 3D warping. MIA 10, 740–751 (2006)
7. Lu, Y., Sun, Y., Liao, R., Ong, S.H.: Registration of pre-operative CT and non-contrast-enhanced C-arm CT: An application to trans-catheter aortic valve implantation (TAVI). In: Lee, K.M., Matsushita, Y., Rehg, J.M., Hu, Z. (eds.) ACCV 2012, Part II. LNCS, vol. 7725, pp. 268–280. Springer, Heidelberg (2013)
8. Jian, B., Vemuri, B.: A robust algorithm for point set registration using mixture of Gaussians. In: IEEE ICCV 2005, vol. 2, pp. 1246–1251 (2005)
9. Rohr, K., Stiehl, H., Sprengel, R., Buzug, T., Weese, J., Kuhn, M.: Landmark-based elastic registration using approximating TPS. TMI 20, 526–534 (2001)
10. Bookstein, F.L.: Principal warps: Thin-plate splines and the decomposition of deformations. IEEE Transactions on Pattern Analysis and Machine Intelligence 11, 567–585 (1989)
11. Richa, R., Poignet, P., Liu, C.: Efficient 3D tracking for motion compensation in beating heart surgery. In: Metaxas, D., Axel, L., Fichtinger, G., Székely, G. (eds.) MICCAI 2008, Part II. LNCS, vol. 5242, pp. 684–691. Springer, Heidelberg (2008)
12. Hermosillo, G., Chefd'Hotel, C., Faugeras, O.: Variational methods for multimodal image matching. IJCV 50, 329–343 (2002)
13. Chefd'hotel, C., Hermosillo, G., Faugeras, O.: Flows of diffeomorphisms for multimodal image registration. In: IEEE ISBI 2002, pp. 753–756 (2002)
14. Murphy, K., Van Ginneken, B., Reinhardt, J., Kabus, S., Ding, K., Deng, X., Cao, K., Du, K., Christensen, G., Garcia, V., et al.: Evaluation of registration methods on thoracic CT: The empire10 challenge. IEEE TMI 30, 1901 (2011)
15. Wang, J., Li, F., Li, Q.: Automated segmentation of lungs with severe interstitial lung disease in CT. Medical Physics 36, 4592 (2009)
16. Miao, S., Liao, R., Pfister, M.: Toward smart utilization of two X-ray images for 2-D/3-D registration applied to abdominal aortic aneurysm interventions. In: IEEE ISBI 2011, vol. 1, pp. 550–555 (2011)
17. Li, C., Jia, X., Sun, Y.: Improved semi-automated segmentation of cardiac CT and MR images. In: IEEE ISBI 2009, pp. 25–28 (2009)